Proc. Natl. Acad. Sci. USA
Vol. 95, pp. 8613–8618, July 1998
Cell Biology

Localization of ADP-ribosylation factor domain protein 1 (ARD1) in lysosomes and Golgi apparatus

NICOLAS VITALE[†‡], KOJI HORIBA[§], VICTOR J. FERRANS[§], JOEL MOSS[†], AND MARTHA VAUGHAN[†]

[†]Pulmonary–Critical Care Medicine Branch and [§]Pathology Section, National Heart, Lung, and Blood Institute, National Institutes of Health, Bethesda, MD 20892

Contributed by Martha Vaughan, May 12, 1998

ABSTRACT **ADP-ribosylation factor domain protein 1 (ARD1) is a member of the ADP ribosylation factor (ARF) family of guanine nucleotide-binding proteins that differs from other ARFs by the presence of a 46-kDa amino-terminal extension which acts as a GTPase-activating protein (GAP) for its ARF domain. Similar to ARF GAPs, the GAP domain of ARD1 contains a zinc finger motif and arginine residues that are critical for activity. It differs from other ARF GAPs in its covalent association with the GTP-binding domain and its specificity for the ARF domain of ARD1. ARFs are presumed to play a key role in the formation of intracellular transport vesicles and in their movement from one compartment to another. We report here that ARD1 overexpressed in cells, as a fusion or nonfusion protein, is localized in vesicular structures that are concentrated mainly in the perinuclear region, but are found also throughout the cytosol. Microscopic colocalization and subcellular fractionation studies showed that ARD1 was associated with the Golgi complex and lysosomal structures. ARD1 expressed as a green fluorescent fusion protein was initially associated with the Golgi network and subsequently localized to lysosomes. Lysosomal and Golgi membranes isolated from human liver by immunoaffinity contained native ARD1. Localization to these organelles, therefore, did not appear to be a result of overexpression. These observations suggest that the ARF-related protein ARD1 may play a role in the formation or function of lysosomes and in protein trafficking between Golgi and lysosomes.**

ADP-ribosylation factors (ARFs) are ≈20-kDa guanine nucleotide-binding proteins recognized as critical components in vesicular trafficking and phospholipase D activation (reviewed in ref. 1). Cells regulate the levels of active and inactive guanine nucleotide-binding proteins by modulating the rates of GDP release, GTP binding, and GTP hydrolysis (GTPase activity). Like other monomeric GTPases, ARFs bind and hydrolyze GTP very slowly. The ratio of ARF-bound GDP to GTP is controlled by guanine nucleotide exchange proteins (GEPs) and GTPase-activating proteins (GAPs), which thereby regulate its activity. Several ARF GEPs and ARF GAPs have been purified and cloned (2). ARF GEPs fall into two families: ≈200-kDa brefeldin A-sensitive and ≈50-kDa brefeldin A-insensitive GEPs (2). ARF GAPs differ in their phospholipid sensitivity and ARF specificity.

ADP-ribosylation factor domain protein 1 (ARD1), is a 64-kDa protein that contains an 18-kDa carboxyl-terminal ARF domain and a 46-kDa amino-terminal domain (3). Like ARFs, the 18-kDa ARF domain of the 64-kDa ARD1 specifically binds GDP and GTP and lacks detectable GTPase activity (4). Using recombinant proteins, it was shown that the 46-kDa amino-terminal domain of ARD1 physically binds to the ARF domain and stimulates hydrolysis of bound GTP (5). The stimulatory effect of the amino-terminal domain on the GTPase activity of the ARF domain is specific, as it did not increase GTP hydrolysis by other members of the ARF family (6). Functional and physical interactions between the GTP-binding and GAP domains required two negatively charged amino acids (Asp427 and Glu428) located in the "effector" region of the ARF domain (7), which probably interact with two positively charged amino acids (Arg249 and Lys250) in the amino-terminal domain (8). By site-specific mutagenesis, it was further demonstrated that, in the amino-terminal GAP domain, an intact zinc finger motif, two arginines, and a sequence that resembles a consensus motif present in Rho/Rac GAPs are required for GAP activity (8).

Localization of ARF1 to the Golgi complex in mammalian cells and the secretion phenotype of yeast with an *arf1*$^-$ mutation, as well as the subsequent identification of ARF1 as a structural component of Golgi-derived coated vesicles, have implicated ARF1 in the process of Golgi transport (reviewed in ref. 9). In contrast, ARF6 has been recently implicated in peripheral vesicular trafficking events such as endocytosis (10, 11) and exocytosis (12, 13).

We report here that ARD1 has a specific subcellular localization, distinct from those of other ARFs. Overexpression of ARD1 in NIH 3T3, COS 7, and HeLa cells resulted in a vesicular localization typical of the Golgi apparatus and the lysosomal compartment. In nontransfected cells, native ARD1 was associated with lysosomal and Golgi membranes.

MATERIALS AND METHODS

Materials. PCR reagents and restriction enzymes were purchased from Boehringer Mannheim, unless otherwise indicated; brefeldin A from Epicentre Technologies (Madison, WI); methyl-(5-[2-thienylcarbonyl]-1*H*-benzimidazol-2-yl)carbamate (nocodazole) from Sigma; DMEM, fetal bovine serum, penicillin/streptomycin solution, and glutamine from Life Technologies (Grand Island, NY); and cells from the American Type Culture Collection. Sources of other materials have been published (4–8).

Construction of an Eukaryotic Expression Vector Containing ARD1. ARD1 cDNA was amplified from a human frontal cortex library (CLONTECH) by PCR in the presence of *Pfu* (Stratagene) with the forward primer 5′-TCCCCT*CTCGAG*ATGGCTACCCTGGTTGTAAAC-3′ (italicized sequence indicates *Xho*I restriction site) and reverse primer 5′-CTGCCT*GGATCC*TCAAGCAACATCCAATACTCCAGC-3′ (italicized sequence indicates *Bam*HI restriction site). Differences from the original clone (European Molecular Biology Laboratory Data Bank 1993, accession no. L04510) are underlined. The forward and reverse primers each introduced five replacement bases, creating *Xho*I and *Bam*HI restriction sites, respectively. The PCR product was extracted from low-melting (LM) agarose gel, puri-

The publication costs of this article were defrayed in part by page charge payment. This article must therefore be hereby marked "*advertisement*" in accordance with 18 U.S.C. §1734 solely to indicate this fact.

0027-8424/98/958613-6$0.00/0
PNAS is available online at http://www.pnas.org.

Abbreviations: AcR, acetate–Ringer's solution (pH 6.6); AP, adaptor protein; ARF, ADP-ribosylation factor; ARD, ARF domain protein; GAP, GTPase-activating protein; GEP, guanine nucleotide exchange protein; GFP, green fluorescent protein; LAMP, lysosome-associated membrane protein; LM, low melting; TGN, trans-Golgi network.

[‡]To whom reprint requests should be addressed at: Room 5N-307, Building 10, National Institutes of Health, Bethesda, MD 20892-1434. e-mail: vitalen@fido.nhlbi.nih.gov.

fied with the Wizard PCR purification kit (Promega), and ligated in-frame to the *Xho*I- and *Bam*HI-digested pcDNA3.1/Zeo(−) expression vector (Invitrogen). Ultracompetent cells (Stratagene) were transformed with the resulting plasmid pcDNA3.1/Zeo(ARD1), which had been purified with the plasmid Maxiprep kit (Qiagen, Chatworth, CA). The entire sequence of the ARD1 construct was confirmed by automated sequencing (373 DNA Sequencer; Applied Biosystems) using the primers 5′-TTATACGACTCACTATAGGG-3′, 5′-AGCTGCAGAAGAATCCATT-3′, 5′-ATCAATTTTAGATATGGCT-3′, 5′-ATGATTGTAGAGTTGTCTT-3′, 5′-TTATTACCTCAATACTCAA-3′, and 5′-GCTAGTTATTGCTCAGCGG-3′. Since expression of ARD1 in transfected NIH 3T3 or COS 7 cells was not detected by Western blotting or immunofluorescence, the original Kozak sequence present in the human clone (3) was introduced by PCR. Plasmid pcDNA3.1/Zeo(ARD1) described above was amplified by PCR in the presence of *Pfu* DNA polymerase (Stratagene), with the forward primer 5′-AG*C*A*G*A*CTCG*GTTCCT**AGGATGG**-3′ and the reverse primer 5′-TAGAAGGCACAGTCGAGG-3′. Differences from pcDNA3.1/Zeo(ARD1) are underlined. The forward primer introduced an *Xho*I restriction site (italicized) as well as the original Kozak sequence (bold face) of ARD1 (European Molecular Biology Laboratory Data Bank 1993, accession no. L04510). The PCR product was extracted from LM agarose gel, purified with the Wizard PCR purification kit (Promega), and ligated in-frame to the *Xho*I- and *Bam*HI-digested pcDNA3.1/Zeo(−) expression vector. Ultracompetent cells (Stratagene) were transformed with the resulting plasmid pcDNA3.1/Zeo(ARD1),¶ which had been purified with the plasmid Maxiprep kit (Qiagen). The entire sequence of the ARD1 construct was confirmed as described above.

Construction of Eukaryotic Expression Vectors Containing ARD1 Fusions. The ARD1 fragment was amplified by PCR in the presence of *Pfu* from pcDNA3.1/Zeo(ARD1) with the forward primer 5′-AGCA*GACTCG*GTTCCTAGGATGG-3′ and the reverse primer 5′-TACTA*GGATCC***TCA**CTTGTCATCGTCGTCCTTGTAGTCAGCCACATCC*AATACTCCAGC-3′ (italicized sequence is a *Bam*HI restriction site, bold sequence is the stop codon, and C* indicates a base replaced to avoid hairpin formation in the primer, resulting in a conservative mutation in ARD1). The reverse primer introduced a FLAG sequence at the 3′ end of ARD1 (underlined). The PCR product after digestion with *Xho*I and *Bam*HI was extracted from LM agarose gel, purified with the Wizard PCR purification kit (Promega), and ligated in-frame to the *Xho*I- and *Bam*HI-digested pcDNA3.1/Zeo(−) expression vector.

The ARD1 fragment was amplified by PCR in the presence of *Pfu* from the pcDNA3.1/Zeo(ARD1) construct with the forward primer 5′-GACTC*GCTAGC***TAGGATGG**CTACCCTGATTGTAAACAAGCTC-3′ (italicized sequence is a *Nhe*I restriction site, bold sequence is the Kozak sequence, and differences from pcDNA3.1/Zeo(ARD1) are underlined). In the reverse primer, 5′-TAGCTA*GGGCCC*AACATCCAATACTCCAGC-3′; italicized sequence is an *Apa*I restriction site, creation of which replaced the C-terminal alanine of ARD1 with glycine. The *Nhe*I–*Apa*I-digested PCR product was extracted from LM agarose gel, purified with the Wizard PCR purification kit (Promega), and ligated in-frame to the *Nhe*I- and *Apa*I-digested pcDNA3.1/myc–His(A) expression vector (Invitrogen).

The ARD1 fragment was amplified by PCR in the presence of *Pfu* from the pcDNA3.1/Zeo(ARD1) construct with forward primer 5′-*AGATCT***CT***ATG*GCTACCCTGGTTGTAAAC-3′ (italicized sequence is a *Bgl*II restriction site; underlined sequence is the initiation codon) and reverse primer 5′-*GTCGAC***T**TCAAGCAACATCCAATACTCCAGCAGC-3′ (italicized sequence is a *Sal*I restriction site and underlined sequence is the termination codon). The bases indicated in bold in both primers maintained the frame for expression in pEGFP-C2. *Taq* DNA polymerase was added during the last cycle of the PCR and the product was cloned into pCR2.1 according to the manufacturer's instructions (TA-cloning; Invitrogen). Plasmid containing the insert was purified with Wizard Plus MiniPrep kit (Promega) and digested with *Bgl*II and *Sal*I. The insert was extracted from LM agarose gel, purified with the Wizard PCR purification kit (Promega), and ligated in-frame to the *Bgl*II- and *Sal*I-digested pEGFP-C2 expression vector (CLONTECH).

Ultracompetent cells (Stratagene) were transformed with the plasmids pcDNA3.1/Zeo(ARD1–FLAG), pcDNA3.1/myc–His(ARD1), and pEGFP-C2(ARD1) and plasmids purified from 200 ml of culture after an overnight growth. Entire sequences of ARD1 constructs were confirmed by automated sequencing.

Antibodies. HPLC-purified (>95% pure) synthetic peptides representing N- and C-terminal sequences of ARD1 (Nt-ARD1: ATLVVNKLGAG; Ct-ARD1: QLVAAGVLDVA) were purchased from Biosynthesis (Lewisville, TX). Mass spectroscopy and amino acid analysis and sequencing were performed on each peptide. Peptides were dissolved in water at a final concentration of 10 mg/ml. Rabbits were immunized with either Nt-ARD1 or Ct-ARD1 peptide coupled to hemocyanin as described previously (14). After $(NH_4)_2SO_4$ precipitation and dialysis, IgG from antisera against the NH_2- and COOH-terminal ARD1 peptides

¶ARD1 constructs with the original Kozak sequence.

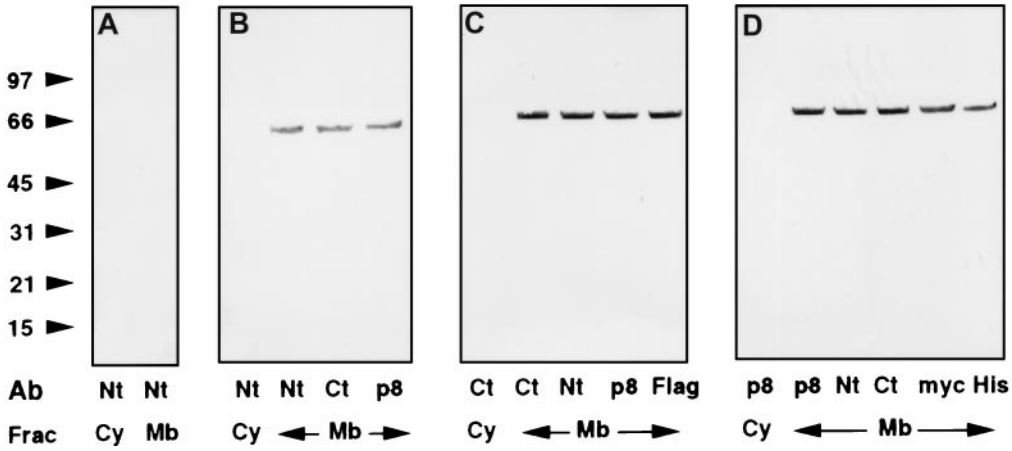

FIG. 1. Localization of ARD1 by Western blotting. Nontransfected NIH 3T3 cells (*A*) or cells transfected with pcDNA3.1(ARD1) (*B*), pcDNA3.1(ARD1–FLAG) (*C*), or pcDNA3.1/myc–His(ARD1) (*D*) were scraped from three 100-mm dishes in 2 ml of ice-cold buffer A [20 mM Tris (pH 7.4), 1 mM EDTA, 0.32 M sucrose, 5 μg/ml each of aprotinin, and leupeptin, 2 μg/ml pepstatin, and 1 mM 4-(2-aminoethyl)-benzenesulfonyl fluoride] and lysed by 15 passages through a 25-gauge needle. Crude membrane and cytosolic fractions were recovered after centrifugation (100,000 × *g*, 30 min) of the postnuclear supernatant. Samples of cytosol (Cy) or total membrane (Mb) proteins (40 μg) were separated by SDS/PAGE in 4–20% gels and transferred to nitrocellulose membranes for Western blotting. Primary antibodies indicated below each lane were diluted as follows: anti-Nt-ARD1, 1:100,000; anti-Ct-ARD1, 1:100,000; anti-recombinant ARD1 (p8) 1:15,000; anti-FLAG, 1:2,000; anti-myc, 1:10,000, and anti-His_6 C-terminal (His), 1:2,000. Alkaline phosphatase-conjugated anti-mouse and anti-rabbit secondary antibodies were diluted 1:3000. The experiment was repeated once with COS 7 cells and identical results were obtained.

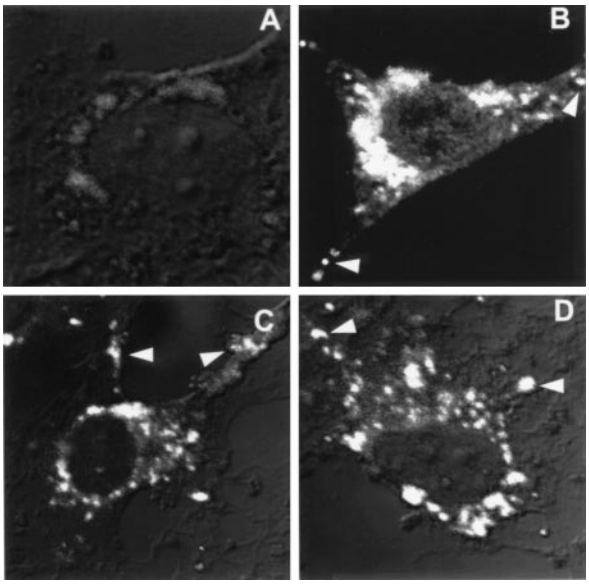

FIG. 2. Intracellular localization of ARD1 by immunofluorescence. NIH 3T3 cells were transfected with pcDNA3.1(ARD1) without a Kozak sequence (*A*), with pcDNA3.1(ARD1) with a Kozak sequence (*B–D*). Immunofluorescence images obtained after incubation of cells with anti-ARD1 (1:1,000) (*A* and *B*), anti-Nt-ARD1 (1:10,000) (*C*), and anti-Ct-ARD1 (1:10,000) (*D*) antibodies are shown. Arrows indicate labeled vesicular structures that are distant from the perinuclear area. Identical results were obtained with at least three different NIH 3T3 cell preparations and with COS 7 and HeLa cells.

was purified on protein A–Sepharose G (Pierce) and then affinity purified on Affi-Gel 15 and Affi-Gel 10 (Bio-Rad) coupled to Nt-ARD1 and Ct-ARD1 peptides, respectively. Specific antibodies were eluted in 12 ml of 0.2 M glycine (pH 2.7)/10% ethylene glycol and the pH was immediately adjusted to 7.5 with 1 M NaOH. After dialysis against PBS, antibodies were concentrated (Centricon 50) and stored at −80°C in 30% glycerol. Polyclonal antibodies against ARD1 were prepared by injecting purified recombinant fusion proteins (glutathione *S*-transferase–ARD1) into rabbits as described (8). The ARD1 antibody was affinity purified on His_6–ARD1–Ni^{2+} columns (Novagen) and stored as described above. Specificity of NH_2- and COOH-terminal and ARD1 antibodies has been demonstrated (8). Antibodies against myc and His C-terminal tags were purchased from Invitrogen and the antibody against FLAG was from Promega. Antibodies against βCOP, p58, and adaptor protein 1 (AP1) were purchased from Sigma, as were the secondary antibodies used for Western blotting and immunofluorescence studies. Antibodies against BiP (anti-grp78) were a gift from Y. Shakur (National Institutes of Health).

Cell Culture and Eukaryotic Expression. NIH 3T3 fibroblasts and COS 7 and HeLa cells were grown in DMEM containing 25 mM glucose, 10% fetal bovine serum, penicillin and streptomycin (each 10 units/ml), and 200 mM glutamine. Absence of *Mycoplasma* in culture was confirmed by PCR using the *Mycoplasma* PCR primer set provided by Stratagene. Expression plasmids with DNA encoding ARD1 were introduced into NIH 3T3, COS 7, or HeLa cells using Transfectam (Promega). Plasmid DNA (5 μg) and Transfectam (20 μl) were diluted separately with DMEM without serum and antibiotics and combined (total vol 3.9 ml) just before addition to cells (100-mm dishes, 80% confluent). After 2 h of incubation at 37°C, 10 ml of culture medium with fetal bovine serum and antibiotics was added. Expression of ARD1 was assessed by Western blotting or immunofluorescence after 48 h, except in the time course experiment (see Fig. 4).

Immunocytochemistry. Cells were fixed for 20 min in 4% paraformaldehyde in 0.12 M sodium/potassium phosphate buffer, pH 7.0 (15). After several rinses with PBS, cells were permeabilized for 4 min in PBS containing 0.1% Triton X-100 (or when indicated, for 10 min in PBS containing 10 μM digitonin) and then incubated for 1 h with 3% BSA and 10% normal goat serum in PBS to reduce nonspecific reaction. Cells were incubated for 1 h with the primary antibody diluted in PBS containing 3% BSA in a moist chamber, washed, and subsequently incubated with the appropriate secondary antibodies diluted to 1:400. Coverslips were then extensively washed with PBS, rinsed with water, and mounted in Mowiol 4-88 (Hoechst Pharmaceuticals). For evaluation of immunofluorescence, samples were inspected with a PlanApo oil immersion objective (×60) on a Nikon ELWD0.3 microscope. Acquisition of confocal images of labeled cells was done essentially as described earlier (15). No staining was observed with secondary antibody alone or when the cells were not permeabilized.

Immunomagnetic Isolation of Lysosomes and Golgi. Membranes from lysosomes and Golgi were purified from crude membranes of human liver (Brain and Tissue Bank, University of Miami, FL) with Dynabeads M-500 (Dynal) according to the manufacturer's instructions. Briefly, 500 μg of rat anti-mouse Fc antibody was bound to 8×10^8 Dynabeads, to serve as linker for either the antibody against lysosomal lysosome-associated membrane protein 1 (LAMP1; 100 μg) or the antibody against Golgi AP1 (80 μg). Crude membranes were prepared by centrifugation (100,000 × *g*, 30 min) of a postnuclear supernatant from human liver homogenate. Twenty micrograms of crude membranes was incubated for 12 h at 4°C with 2×10^8 Dynabeads. The beads were then washed five times each with 1 ml of ice-cold PBS containing 5% BSA, PBS with 0.1% BSA, and PBS. Molecules bound to beads were eluted in 1 ml of 0.2 M glycine(pH 2.7)/10% ethylene glycol and the pH was immediately adjusted to 7.0 with 1 M Tris. Antibodies were bound to protein A–Sepharose G (Pierce) and the remaining solution was dialyzed against PBS and concentrated (Centricon 10). Protein was estimated by a dye-binding assay (16). Samples (20 μg) were subjected to SDS/PAGE in 4–20% gels and transferred to nitrocellulose membrane for Western blotting. Procedures for electrophoretic transfer and immunological detection have been described (17).

RESULTS

Because we had failed to detect ARD1 in crude cytosolic or membrane fractions from mammalian tissue (data not shown) or cultured cells (Fig. 1*A*), we induced overexpression of recombinant ARD1 in NIH 3T3 cells to identify its intracellular localization. As shown in Fig. 1*B*, antibodies raised against the amino-terminal decapeptide (Nt-ARD1), the carboxyl-terminal decapeptide (Ct-ARD1), or recombinant ARD1 (p8) detected a single protein in the membrane fraction but not in the cytosol. The apparent molecular mass of the product was 64 kDa, identical to that of the recombinant protein. To test the specificity of the antibodies, we induced overexpression of ARD1 in NIH 3T3 cells as fusion proteins with FLAG (Fig. 1*C*) or myc–His (Fig. 1*D*) epitopes at the C terminus. As expected FLAG (Fig. 1*C*), myc or His (Fig. 1*D*) antibodies, as well as N-terminal, C-terminal, or ARD1 (p8) polyclonal antibodies, recognized a single product in the membranes of cells transfected with pcDNA3.1(ARD1–FLAG) and pcDNA3.1/myc–His(ARD1), respectively. The mobility of the products was, however, slightly less than those of the nonfusion products, presumably because of the presence of the additional tag sequences. These results confirmed the specificity of the N-terminal, C-terminal, and ARD1 polyclonal antibodies and suggested that ARD1 was membrane associated.

The intracellular localization of the 64-kDa ARD1 protein was investigated in transfected NIH 3T3, COS 7, and HeLa cells by confocal laser scanning microscopy using ARD1-specific antibodies and antibodies against epitope tags. Nontransfected cells, mock-transfected cells (data not shown), and cells transfected with pcDNA3.1(ARD1) lacking the original Kozak sequence (Fig. 2*A*) were not labeled by anti-ARD1 antibodies (Fig. 2*A*). When the original Kozak sequence was present, however, anti-

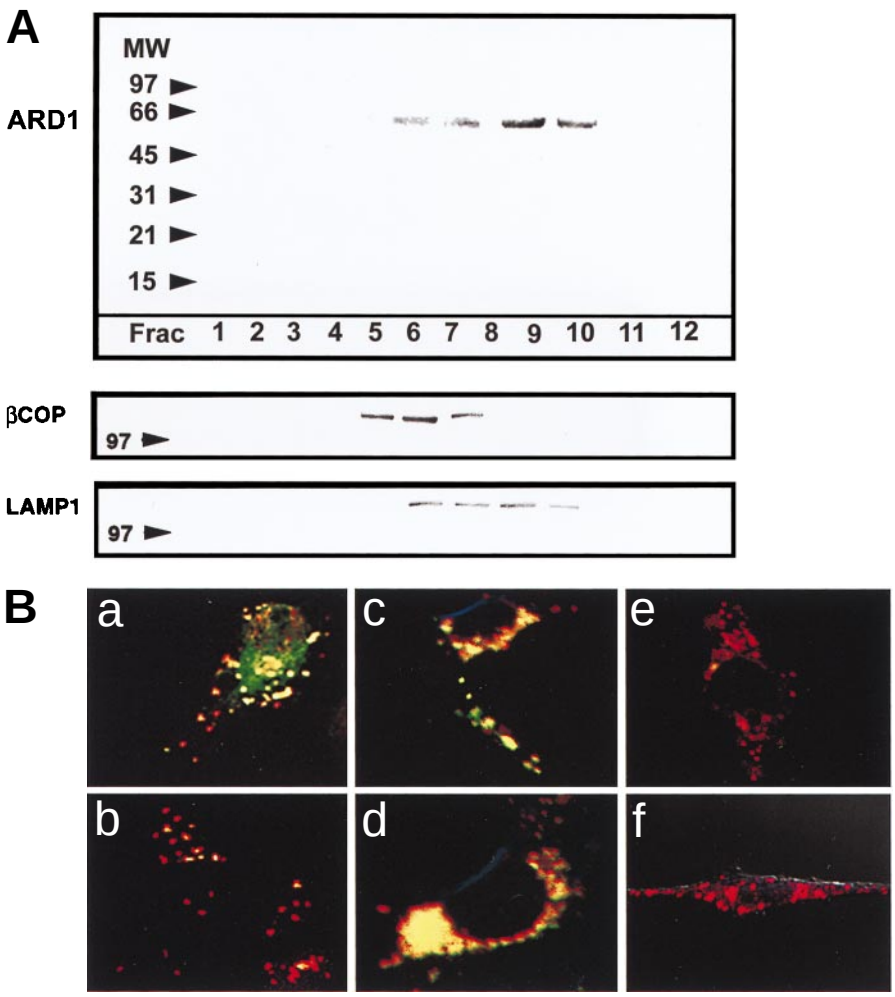

FIG. 3. Subcellular localization of ARD1. (*A*) Subcellular fractionation of cells overexpressing ARD1. Five 100-mm dishes of HeLa cells were transfected with pcDNA(ARD1). After 48 h, cells were homogenized in 2 ml of buffer A (see legend for Fig. 1) and crude membranes were obtained by centrifugation at 100,000 × *g* for 30 min as described in Fig. 1. Membranes were layered on a continuous sucrose density gradient [1–2.2 M sucrose and 10 mM Tris (pH 7.4)] as described (17) and centrifuged for 1 h at 100,000 × *g*. Twelve 1-ml fractions were collected from the top and diluted in 20 mM Tris (pH 8.0) with 1 mM EDTA; membranes were collected by centrifugation (30 min at 100,000 × *g*) of each fraction and protein was assayed according to the Bradford procedure (16). The distribution of membranes on the gradient has been described (14, 17). Samples of proteins (40 μg) from each fraction were subjected to SDS/PAGE, transferred to nitrocellulose membranes, and reacted with antibodies against Nt-ARD1 (1:10,000), βCOP (1:200), or LAMP1 (1:1,000). Positions of protein standards (kDa) are on the left. (*B*) Intracellular distribution of ARD1 by immunofluorescence. COS 7 cells transfected with pcDNA3.1(ARD1) were incubated with 4 ml of warm (37°C) DMEM (*a*) or DMEM containing brefeldin A, 10 μg/ml (*b*) for 10 min, then incubated simultaneously with the rabbit anti-Nt-ARD1 (1:10,000) and the mouse anti-p58 (1:100) antibodies, followed by anti-rabbit IgG–rhodamine and anti-mouse IgG–fluorescein isothiocyanate antibodies. Transfected HeLa cells were incubated with the rabbit anti-Nt-ARD1 (1:15,000) (*c–d*) and the mouse anti-LAMP1 (1:1,000) (*c*) followed by secondary antibodies. Some cells were incubated for 1 h with 60 nM Lysotracker (lysosomal marker) in DMEM before fixation and permeabilization with digitonin (*d*). Transfected NIH 3T3 cells were incubated at 37°C for 15 min in AcR solution (19) (*e*) or nocodazole, 5 μg/ml, for 60 min (*f*) before immunostaining. Results have been repeated at least once with different cell preparations.

ARD1 (Fig. 2*B*), Nt-ARD1 (Fig. 2*C*), and Ct-ARD1 (Fig. 2*D*) antibodies stained strongly the perinuclear region. Some individual vesicular structures were also labeled. These structures could be found throughout the cytosol, sometimes in cellular protrusions far from the perinuclear area (arrows in Fig. 2 *B–D*). Incubation of antipeptide antibodies or the anti-ARD1 antibody with the appropriate Nt-ARD1 or Ct-ARD1 peptide or recombinant ARD1 protein prevented subsequent staining of the perinuclear and vesicular structures (data not shown). Localization of ARD1 in the perinuclear region and in vesicular structures was also observed in cells expressing ARD1–FLAG or ARD1–myc–His stained with FLAG or myc antibodies, respectively (data not shown).

The perinuclear region contains many different organelles, including endoplasmic reticulum, Golgi, the microtubule-organizing center, and vesicular structures of the endosome–lysosome system. To identify precisely the subcellular localization of ARD1, subcellular fractionation on continuous sucrose density gradients and dual-staining immunofluorescence experiments utilizing confocal microscopy were carried out. Crude membranes from HeLa cells overexpressing ARD1 were separated on a sucrose density gradient and the distribution of ARD1 was estimated by immunoreplica analysis (Fig. 3*A*). A single product with a molecular mass of ≈64 kDa was detected in fractions 6–9 of the gradient (Fig. 3*A*, *Top*), whereas the trans-Golgi network (TGN)-associated protein βCOP was found in fractions 5–7 (Fig. 3*A*, *Middle*) and the lysosomal protein LAMP1 in fractions 6–9 (Fig. 3*A*, *Bottom*). These results indicated that ARD1 is present in fractions that contain Golgi and lysosomal membranes and could be associated with these organelles.

In double immunofluorescence experiments with anti-ARD1 antibodies and organelle-specific antibodies or a fluorescent probe for these organelles, the yellow staining pattern obtained from the superimposed images of ARD1-rhodamine and p58–fluorescein isothiocyanate (Golgi marker) fluorescence revealed partial colocalization of ARD1 with p58 in COS 7 cells (Fig. 3*Ba*). However, vesicular structures that were labeled by antibodies against ARD1 were not stained with antibodies against the Golgi complex and not all of the Golgi components were labeled by the ARD1 antibodies. Identical results were obtained in NIH 3T3 cells with antibodies against TGN markers such as AP1 and βCOP (data not shown), suggesting that ARD1 was indeed partially associated with the TGN, but was also present on other structures. In agreement with these results is the observation that ARD1-positive structures, in brefeldin A-treated cells, were for the most part not labeled by antibodies to components of the Golgi complex such as anti-p58 (Fig. 3*Bb*), anti-βCOP, or anti-AP1 (data not shown). Since brefeldin A disrupts the Golgi apparatus (18), the structures that were labeled by ARD1 antibodies and were not affected by the brief brefeldin A treatment, and were present in cellular extensions, are likely not to be Golgi membranes. Colocalization of ARD1 with two lysosomal markers, LAMP1 (Fig. 3*Bc*) and the fluorescent probe Lysotracker (Fig. 3*Bd*) suggested that ARD1 was also associated with lysosomes. Incubation of cells in an acidic acetate Ringer's medium (AcR) or treatment with nocodazole, which are known to cause dispersion of lysosomes from the perinuclear area (19, 20),

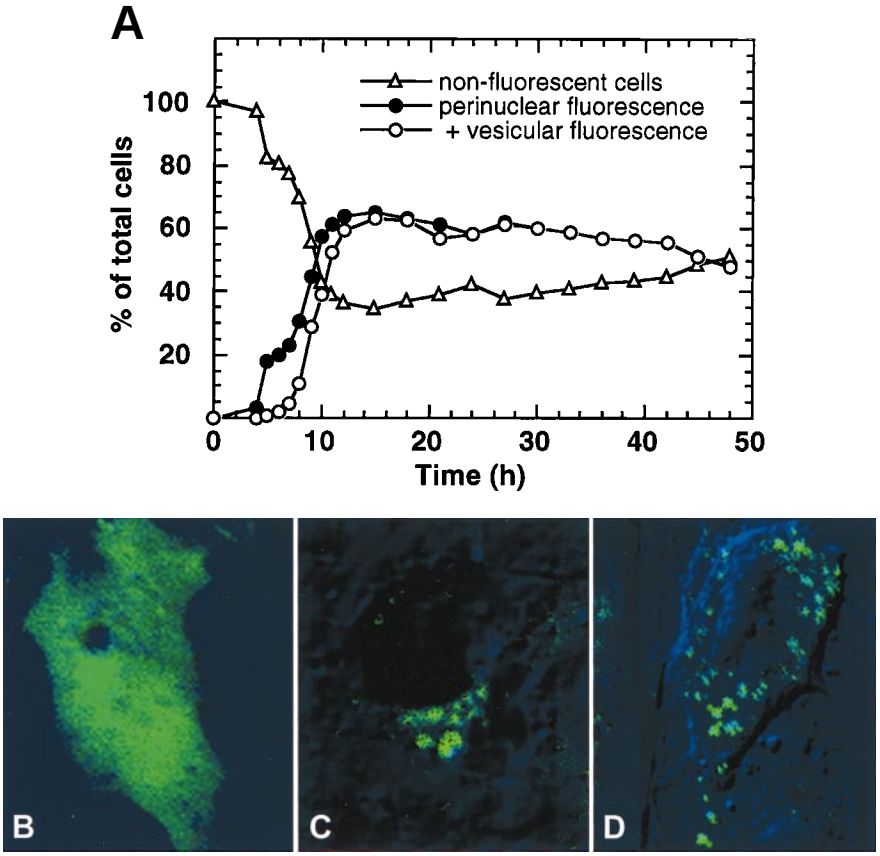

FIG. 4. Time course expression of ARD1. NIH 3T3 cells were transfected with pEGFP-C2(ARD1) for 2 h in DMEM before culture medium with fetal bovine serum and antibiotics were added. At the indicated time after initiation of transfection, cells were incubated for 15 min at 37°C with AcR and coverslips were briefly washed with PBS before microscopic observation of living cells. Alternatively, cells were fixed and mounted before microscopy. Identical conclusions were obtained with the two procedures. (*A*) Cells in a planar section randomly selected were inspected and numbers of cells displaying green fluorescence in the perinuclear area and in scattered cytoplasmic vesicular structures were recorded. Cells in each category are reported as a percentage of the total number of cells counted per coverslip, which was between 217 and 380. Cell density increased slightly during the 48 h of the experiment. (*B*) NIH 3T3 cells expressing the cytosolic GFP 12 h after transfection. (*C*) NIH 3T3 cell expressing GFP-ARD1 5 h or (*D*) 12 h after transfection and after AcR treatment. Identical results were obtained with two different cell cultures.

induced dispersion of the ARD1 staining (Fig. 3*Be* and *f*, respectively). Finally, no colocalization of ARD1 staining with actin, tubulin, or the endoplasmic reticulum marker BiP was found (data not shown). All together these results are strong evidence that recombinant ARD1 is associated with lysosomes and to a lesser extent with the Golgi apparatus.

We investigated the time course of recombinant ARD1 expression using green fluorescent protein (GFP)-ARD1 after treatment of cells with AcR medium. Six hours after transfection, GFP–ARD1 was detected in only about 20% of the cells (Fig. 4*A*). In all cells expressing recombinant protein, however, after the acidic treatment fluorescence was restricted to the perinuclear region, presumably associated with Golgi membranes (Fig. 4 *A* and *C*). Seven hours after transfection and after the brief AcR treatment, the number of cells expressing ARD1 in the Golgi complex had increased, but more interestingly, some cells contained, in addition, scattered fluorescent structures dispersed in the cytosol (Fig. 4 *A* and *D*), suggesting that ARD1 was then also present in lysosomes. After 14 h, 62% of cells expressed GFP–ARD1 and after 18 h, virtually every transfected cell expressed ARD1 in both the Golgi complex and lysosomes (Fig. 4*A*). These results are consistent with the conclusion that ARD1 initially appears in the Golgi apparatus and is then transported to the lysosomes. The data from the dual staining experiments, however, showed that, at steady state, ARD1 was present in both the Golgi complex and the lysosomes, consistent with the possibility that it might cycle between the two organelles.

Since it appeared that overexpressed ARD1 was present in Golgi and in lysosomes, we looked for native ARD1 in purified organelles from human tissue. From a human liver library, we cloned (Fig. 5*A*) and sequenced an ARD1 cDNA that was identical in sequence to that of ARD1 cloned earlier from human fetal brain (3). Purification of Golgi and lysosomes membranes from human liver to near homogeneity was achieved by using specific antibodies that were directed against the Golgi complex (AP1) or lysosomes (LAMP1) and were linked to magnetic beads (Dynabeads). Membranes purified with LAMP1 beads contained the lysosomal protein LAMP2 (Fig. 5*B*, lane 1), but not the Golgi marker p58 (Fig. 5*B*, lane 2), or markers for other subcellular structures such as Gαs, actin, BiP, and tubulin (data not shown), suggesting that they were highly enriched in lysosomal membranes. Conversely, membranes purified with AP1 antibodies stained only with anti-p58 (Fig. 5*C*, lanes 1 and 2), indicating that they were mainly from Golgi. Both lysosomal and Golgi membranes contained a single protein of ≈64 kDa that reacted with antibodies against Nt-ARD1 and Ct-ARD1 (Fig. 5*B*, C, lanes 3 and 4), suggesting that ARD1 was present in both organelles. The antibody raised against the recombinant ARD1 protein (p8) also detected ARD1 from lysosomal membranes, but not from Golgi membranes (Fig. 5 *B* and *C*, lanes 5), presumably because the amount of ARD1 was higher in lysosomal than in Golgi membranes.

DISCUSSION

Exciting progress has recently been made in understanding the protein machinery responsible for the formation, targeting, and fusion of vesicles along the secretory pathway. Most of the developing models emphasize the similarity in proteins and mechanisms underlying the multiple steps of intracellular vesicular transport. In these models, key roles are assigned to both monomeric and trimeric guanine nucleotide-binding proteins because of the presence of specific guanine nucleotide-binding proteins, in particular vesicular structures, and because their cyclic activation and inactivation by GTP and GDP, respectively, could control the formation and functioning of docking and fusion complexes. Families of guanine nucleotide-binding proteins known to be involved in trafficking include the diverse ARF, Rab, Rac, Ras, and Rho families of ≈20-kDa GTPases, novel GTPases such as dynamin, and many of the Gα or βγ subunits of heterotrimeric G proteins (review in ref. 21). To our knowledge, there is no evidence for GTPase involvement directly in trafficking to or from the lysosomal compartment. Evidence presented

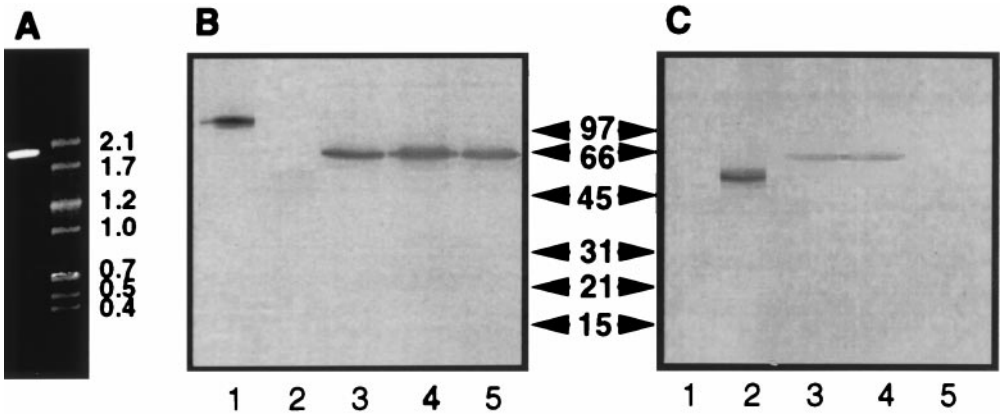

FIG. 5. Identification of ARD1 mRNA and protein from normal tissue. (*A*) Four hundred nanograms of a human liver cDNA library (Origene Technologies, Rockville, MD) was used as a template for PCR with forward primer 5′-GGCGCTTCCCCTGCGAGGATGGCTACCCTG-3′ (initiation codon is underlined) and reverse primer 5′-CAACTGCTGCCTTTAAAATCAAG-CAACATC-3′ (stop codon is underlined). A single product of ≈1.9 kb was obtained. Positions of size markers (kb) are indicated. The product was cloned into TA–vector (Invitrogen) according to the manufacturer's instruction and sequenced as described earlier (7). Samples of proteins (20 μg) from affinity-purified lysosomal (*B*) or Golgi (*C*) membranes were separated by SDS/PAGE in 4–20% gels and transferred to nitrocellulose for reaction with anti-LAMP2 (1:200, lane 1), anti-p58 (1:100, lane 2), anti-Nt ARD1 (1:1000, lane 3), anti-Ct ARD1 (1:1000, lane 4), and anti-ARD1 (1:200, lane 5) antibodies. Similar results were obtained with two different human livers.

here indicates that ARD1 is associated with the Golgi apparatus (probably the TGN) and with structures of the lysosomal system, suggesting that ARD1 might be involved in transport between these two organelles.

The presence of ARD1 in lysosomes, especially in cells overexpressing the recombinant protein, could of course be explained by the degradation of an overexpressed protein. We believe that this is unlikely for several reasons. First, degradation fragments of ARD1 were never detected by immunoreplica analysis. Second, the pattern of distribution of ARD1 was not affected qualitatively or quantitatively by treatment of cells for 4 h with either 100 μM chloroquine, 10 mM ammonium chloride, or 10 mM methylamine (data not shown), all of which are known to inhibit lysosomal activity. Third, cotransfection of ARD1 and the Golgi-associated ARF3 revealed partial colocalization of the two proteins in the Golgi, but ARF3 was not detected in the ARD1-positive lysosomal structures (data not shown), consistent with the conclusion that overexpression was not driving ARD1 to lysosomes. Finally, detection of ARD1 on LAMP1/2-containing membranes from human liver indicated that native ARD1 was associated with lysosomes in those cells.

The repertoire of activities of the lysosomal system extends beyond its function in degrading biological macromolecules for energy disposal or recycling purposes. Indeed, controlled shifts in lysosomal activity help cells regulate their cytoplasmic volume and growth and remodel local cellular domains (22). Interest in the endosomal–lysosomal system is now entering a new era, sparked in part by suspected roles in Alzheimer's disease, in the propagation of prion diseases, and in the metastatic spread of certain cancers (23). Although transport to lysosomes was originally thought to be unidirectional, today it is abundantly clear that molecules are also leaving the lysosomal system for the plasma membrane or the Golgi apparatus (24). Some of these transport steps require the formation of clathrin-coated vesicles. Clathrin coats also contain adaptor complexes (AP1–3) which mediate clathrin attachment and recruit membrane proteins that selectively localize in clathrin-coated regions (reviewed in ref. 25). Although degenerate, the short tetrapeptide containing tyrosine in the sequence YXXθ (X, any amino acid; θ, hydrophobic amino acid) was demonstrated to be necessary and sufficient for concentration at clathrin-coated pits (26). Partial colocalization of ARD1 and AP1 (N.V., J.M., and M.V., unpublished observation) suggests that ARD1 might interact also with AP1. We are currently investigating the importance of the two YXXL sequences in the ARF domain of ARD1 for its localization and its potential interaction with adaptor proteins.

Molecular evidence shows that newly synthesized molecules are introduced into late lysosomes not by a direct Golgi-to-lysosomes route, but rather indirectly via the prelysosomal compartment (24). Although prelysosomal vesicles can be distinguished from late lysosomes, debate continues over whether they represent a stable, preexisting compartment or a transient intermediate that evolves from early endosomes. It will now be very interesting to investigate the possible involvement of ARD1 in vesicular trafficking events between the Golgi apparatus and the lysosomes or within the lysosomal complex. Because timing is critical in the formation and the activation/deactivation of the fusion complex, it is also very tempting to speculate that the intrinsic GTPase activity of ARD1 could play a fundamental role in the regulation of this transport pathway.

We thank Dr. V. C. Manganiello for critical review of the manuscript, Dr. W. Patton for stimulating discussions, and Dr. Y. Shakur for comments on immunocytochemistry and for the gift of the BiP antibody. We also thank Dr. E. Meacci for the gift of the hARF3 clone and Michael Spencer for his expertise in art work.

1. Moss, J. & Vaughan, M. (1995) *J. Biol. Chem.* **270,** 12327–12330.
2. Moss, J. & Vaughan, M. (1998) *J. Biol. Chem.*, in press.
3. Mishima, K., Tsuchiya, M., Nightingale, M. S., Moss, J. & Vaughan, M. (1993) *J. Biol. Chem.* **268,** 8801–8807.
4. Vitale, N., Moss, J. & Vaughan, M. (1997) *J. Biol. Chem.* **272,** 3897–3904.
5. Vitale, N., Moss, J. & Vaughan, M. (1996) *Proc. Natl. Acad. Sci. USA* **93,** 1941–1944.
6. Ding, M., Vitale, N., Tsai, S.-C., Moss, J. & Vaughan, M. (1996) *J. Biol. Chem.* **271,** 24005–24009.
7. Vitale, N., Moss, J. & Vaughan, M. (1997) *J. Biol. Chem.* **272,** 25077–25082.
8. Vitale, N., Moss, J. & Vaughan, M. (1998) *J. Biol. Chem.* **273,** 2553–2560.
9. Donaldson, J. G. & Klausner, R. D. (1994) *Curr. Opin. Cell Biol.* **6,** 527–532.
10. D'Souza-Schorey, C., Li, G., Colombo, M. I. & Stahl, P. D. (1995) *Science* **267,** 1175–1178.
11. Radhahrishna, H. & Donaldson, J. G. (1997) *J. Cell Biol.* **139,** 49–61.
12. Galas, M.-C., Helms, J. B., Vitale, N., Thiersé, D., Aunis, D. & Bader M.-F. (1997) *J. Biol. Chem.* **272,** 2788–2793.
13. Caumont, A.-S., Galas, M.-C., Vitale, N., Aunis, D. & Bader M.-F. (1998) *J. Biol. Chem.* **273,** 1373–1379.
14. Vitale, N., Mukai, H., Rouot, B., Thiersé, D., Aunis, D. & Bader, M.-F. (1993) *J. Biol. Chem.* **268,** 14715–14723.
15. Chasserot-Golaz, S., Vitale, N., Sagot, I., Delouche, B., Dirrig, S., Pradel, L.-A., Henry, J.-P., Aunis, D. & Bader M.-F. (1996) *J. Cell Biol.* **133,** 1217–1236.
16. Bradford, M. M. (1976) *Anal. Biochem.* **72,** 248–254.
17. Vitale, N., Gensse, M., Chasserot-Golaz, S., Aunis, D. & Bader, M.-F. (1996) *Eur. J. Neurosci.* **8,** 1275–1285.
18. Donaldson, J. G., Lippincott-Schwartz, J., Bloom, G. S., Kreis, T. E. & Klausner, R. D. (1990) *J. Cell Biol.* **111,** 2295–2306.
19. Matteoni, R. & Kreis, T. E. (1987) *J. Cell Biol.* **105,** 1253–1265.
20. Heuser, J. (1989) *J. Cell Biol.* **108,** 855–864.
21. Stow, J. L. (1995) *Curr. Opin. Nephrol. Hypertens.* **4,** 421–425.
22. Kornfeld, S. & Mellman, I. (1989) *Annu. Rev. Cell Biol.* **5,** 483–525.
23. Nixon, R. A. & Catalo, A. M. (1995) *Trends Neurosci.* **18,** 489–496.
24. Storrie, B. & Desjardins, M. (1996) *BioEssays* **18,** 895–903.
25. Mellman, I. (1996) *Annu. Rev. Cell Dev. Biol.* **12,** 575–625.
26. Trowbridge, I. S., Collawn, J. F. & Hopkins, C. R. (1993) *Annu. Rev Cell Biol.* **9,** 129–161.